Whole genome DNA methylation and mutational profiles identify novel changes in proliferative verrucous leukoplakia

Eyituoyo Okoturo, FWACS, FICOMS,[a,b,1] Daniel Green, PhD,[c,1] Kim Clarke, PhD,[c]
Triantafyllos Liloglou, BSc, PhD, FHEA,[a,d] Mark T. Boyd, BSc, PhD, SFHEA, FRSB,[a]
Richard J. Shaw, MD, FDS, FRCS (OMFS), BDS, MBChB (Hons),[a] and Janet M. Risk BSc, PhD[a]

Objective. Proliferative verrucous leukoplakia (PVL) is a rare form of oral leukoplakia with a relatively high transformation rate resulting in oral squamous cell carcinoma (OSCC). Molecular analysis of PVL at the genome level is limited and has only identified molecular similarities between PVL and OSCC. However, the clinical profile of PVL suggests that molecular differences may be more important.

Study Design. Whole exome sequencing of 5 PVL-associated OSCC (PVL-OSCC) and paired blood samples was used to identify somatic mutations common to the tumors. Whole methylome analysis of samples from 4 PVL-associated OSCC and 3 OSCC of non-PVL origin samples was conducted to explore differential methylation.

Results. In contrast to conventional OSCC, PVL-associated OSCC showed infrequent *TP53* mutation and altered spectra of *PIK3CA* and *NOTCH1* mutations. Unsupervised hierarchical clustering identified 63 probes that discriminated between PVL-associated OSCC and OSCC of non-PVL origin. Differences in methylation were most significant for divalent metal ion transport, particularly calcium movement.

Conclusions. Specific differences in mutation and methylation profiles between PVL-derived OSCC and OSCC of non-PVL origin suggest differences in their transformation pathways. Further studies of early PVL lesions may identify markers of transformation that are also applicable to more common oral premalignant disorders such as oral epithelial dysplasia. (Oral Surg Oral Med Oral Pathol Oral Radiol 2023;135:893−903)

Proliferative verrucous leukoplakia (PVL) is a rare form of oral leukoplakia first described in 1985 by Hansen et al.[1] The clinical course begins with an isolated oral white plaque that becomes multifocal and exophytic, often inexorably progressing over decades. The plaque is persistent, irreversible, and refractory to treatment, eventually undergoing malignant transformation to verrucous, followed by invasive, oral squamous cell carcinoma (OSCC) in >50% of cases.[1,2] Despite the high rate of malignant transformation, overall survival in PVL-associated OSCC (PVL-OSCC) is significantly better than that for conventional OSCC.[3]

Diagnosis of PVL is based on a number of clinical and histopathological criteria and is frequently established retrospectively after malignancy has been diagnosed.[1] Several critical clinical features distinguish PVL from other head and neck mucosal lesions at risk of malignant transformation.[4] The very high rate of malignant transformation in PVL, well over 50% in most series,[5] contrasts with that of oral epithelial dysplasia (OED), which is only approximately 10% for mild to moderate dysplasia and 24% for severe dysplasia and carcinoma in situ.[6] Furthermore, PVL generally occurs independently of known risk factors for OSCC and is unrelated to smoking history, alcohol consumption, or high-risk HPV.[7]

The molecular pathogenesis of PVL represents an intriguing and largely uncharted field of investigation. We have speculated that PVL would transform in all patients if given sufficient natural lifespan and observation.[7] The clinical and pathological appearance and

Statement of Clinical Relevance

Proliferative verrucous leukoplakia, a potentially premalignant oral disorder with a high rate of transformation, shows a novel spectrum of mutations and differences in genome methylation compared with conventional oral squamous cell carcinoma that may provide insight into its discrete etiology.

Eyituoyo M. Okoturo and Daniel Green contributed equally to this manuscript.

[a]Liverpool Head and Neck Centre, William Henry Duncan Building, University of Liverpool, Liverpool, UK.
[b]Head and Neck Cancer Division, Oral and Maxillofacial Surgery Department, and Molecular Oncology Program, Medical Research Centre, Lagos State University College of Medicine, Ikeja, Lagos, Nigeria.
[c]Computational Biology Facility, Liverpool Shared Research Facilities, University of Liverpool, Crown Street, Liverpool, UK.
[d]Edge Hill University, Medical School, St Helens Road, Ormskirk, Lancashire, UK.
Corresponding author. E-mail address: J.M.Risk@liverpool.ac.uk

[1]Both made equal contribution to this work.

Received for publication Oct 10, 2022; returned for revision Jan 9, 2023; accepted for publication Mar 6, 2023.

2212-4403/$-see front matter
https://doi.org/10.1016/j.oooo.2023.03.004

progression of PVL to OSCC is highly stereotyped, following a predictable stepwise continuum. As such, it is possible that PVL follows a distinct molecular origin and pathway compared to conventional OSCC or OED. Critical genetic or epigenetic determinants may be unique to PVL or much less commonly seen in comparable The Cancer Genome Atlas (TCGA) metadata relating to head and neck SCC. Given the inexorable progression of PVL to OSCC, we hypothesized that the critical event in malignant transformation is present even in early lesions before the development of epithelial dysplasia.

Recent systematic reviews of the molecular pathogenesis of PVL[8,9] concluded that only aneuploidy showed promise as a putative malignancy marker and highlighted most previous studies' candidate gene approach. Evidently, these studies have been limited by their methodology to targeting aberrations commonly found in OSCC. Only recently have 2 studies of genome-wide studies of PVL exploited the power of contemporary sequencing approaches.[10,11] These 2 related studies investigated differential gene expression and DNA methylation in a small cohort of PVL patients for comparison to the normal oral mucosa. They then validated their results *in silico* against the expression data for 314 specimens and 31 adjacent normal samples from the 2015 TCGA OSCC sample set in which they demonstrated similar expression profiles.[10]

In contrast to these studies, we aimed to investigate the genome-wide and epigenome-wide characteristics of PVL-associated OSCC (PVL-OSCC) and identify where the pattern of DNA methylation or somatic mutations contrasted with conventional OSCC. We hypothesized that this research might give novel insights into the molecular mechanism of malignant transformation in OSCC.

MATERIALS AND METHODS

Patients

Patients with PVL-OSCC were identified from cases observed at the Oral Dysplasia Clinic of the Liverpool University Dental Hospital between 2008 and 2017 (Table I). A diagnosis of PVL was defined as a progressive clinical course based on Hansen's histological grading[1] with numerous biopsy episodes, post-excisional recurrence, and a propensity to develop into OSCC. The histopathology of the biopsied material was re-examined, and cases with an uncertain diagnosis of PVL were excluded, leaving 22 patients. After giving written informed consent, patients were included in this study, which had been approved by the Research Ethics Committee (EC 47.01 and H/10/1002).

Control cases were taken from a previously used cohort of OSCC samples (Research Ethics Committee number 07/Q1505/15[12]) (Table I). Archival formalin-fixed paraffin-embedded (FFPE) tissue was used for single gene confirmatory assays because it was comparable to the format of most of the PVL material. Formalin-fixed paraffin-embedded tissue was available for 20 cases, and an additional 5 cases were available as fresh tissue. These cases are herein referred to as conventional OSCC (cOSCC) samples.

Samples

Following surgery, 5 mm^3 fresh tissue was obtained from within the tumor of PVL-OSCC and cOSCC samples without any necrotic area or tumor margins. Tissue with a histopathologically low Hansen grade (grade 1 to 3) were taken from the same or separate resections performed on the same day and termed low-grade PVL (LG-PVL). The tissue was snap-frozen and stored at -80°C. Paired blood samples were taken as controls for whole exome analysis. Genomic DNA from all fresh frozen samples was extracted using a DNEasy blood and tissue kit (Qiagen LLC, Germantown, MD, USA) according to the manufacturer's protocol. Formalin-fixed paraffin embedded tissue from PVL and cOSCC cases was obtained from the local Pathology department. Genomic DNA was extracted using a DNA FFPE Tissue kit (Qiagen) according to the manufacturer's protocol.

Whole Exome Sequencing

Genomic DNA from 5 fresh, frozen PVL-OSCC cases (Table I) with paired blood samples were subjected to whole exome sequencing (WES) at the Centre for Genomic Research, University of Liverpool, Liverpool, UK. Target capture and library construction were performed using SureSelect Human All Exon v7 (Agilent Technologies, Santa Clara, CA, USA). The libraries were sequenced on an Illumina Hiseq 4000 platform (Illumina Inc., San Diego, CA, USA).

All reads were aligned to the reference genome (WG38) using a Burrows–Wheeler Aligner.[13] Somatic variants were identified by subtracting those detected in the paired blood sample genome sequence using Strelka2[14] with a base call quality score of 90% and a minor allele frequency $\leq$1.0.

Whole Genome Methylation Profiling

Genomic DNA was isolated from fresh frozen samples obtained from 4 PVL-OSCC, 3 cOSCC, and 4 premalignant PVL samples. Two of the premalignant PVL samples were obtained from resection tissue adjacent to 2 of the PVL-OSCC samples (Table I). The DNA samples were transferred to Edinburgh Genomics for bisulfite treatment and genome-wide microarray hybridization using an Infinium MethylationEPIC (EPIC) CytoSNP-850K BeadChip (Illumina).

Table I. Patient cohort

Patient group	*Identifier*	*OSCC* sample*	*WGA† OSCC*	*LG-PVL* sample*	*WGA† LG-PVL*	*Sex*	*Age at first tumor*	*Tumor site*	*PVL lesion extent*
PVL	3328	Y	WES	Y	WGMP	F	64	mandibular alveolus	mandibular gingiva
	4146	Y	WES	Y	WGMP	F	77	FOM	panoral
	4107	Y	WES			F	75	lateral tongue	panoral
	3275	Y	WES/WGMP	Y		F	69	buccal	buccal
	3576	Y	WES/WGMP	Y	WGMP	M	61	FOM	panoral
	3390	Y	WGMP	Y	WGMP	F	70	ventral tongue	hypopharynx
	4244	Y	WGMP			F	95	lateral tongue	panoral
	3002	Y		Y		M	40	FOM	panoral
	3114	Y		Y		F	63	buccal	panoral
	3144	Y		Y		F	80	soft palate	hypopharynx/buccal
	3287	Y		Y		M	42	lateral tongue	lateral tongue
	3294	Y		Y		F	66	hard palate	buccal/hard palate
	3343	Y		Y		F	70	buccal/soft palate	buccal
	3265	Y				F	89	BOT/lingual tonsil	buccal/FOM
	3450	Y				M	60	mandibular alveolus	panoral
	3698	Y		Y		M	72	mandibular alveolus	panoral
	3866	Y				F	85	lateral tongue	panoral
	3906	Y				M	35	buccal	buccal
	3935	Y		Y		M	57	FOM	FOM
	3936			Y		M	N/A		FOM
	3406			Y		M	N/A		mandibular alveolus/gingiva
	4224	Y				F	42	lateral tongue	panoral
TOTAL		20		15					
cOSCC	3314	Y	WGMP			M		FOM	
n = 25	3269	Y	WGMP			M	66	alveolus	
	3276	Y	WGMP			M	59	FOM	
	3327	Y				M	67	tonsil	
	3329	Y				M	48	FOM	
	3330	Y				M	59	lateral tongue	
	3334	Y				M	64	maxilla	
	3335	Y				M	64		
	3336	Y				M	57	mandibular alveolus	
	3337	Y				M	53	soft palate	
	3338	Y				M	50	ventral tongue	
	3345	Y				M	76	tongue	
	3346	Y				M	76	ventral tongue	
	3347	Y				M	65	mandibular alveolus	
	3350	Y				F	89	mandibular alveolus	
	3352	Y				M	75	FOM	
	3354	Y				F	48	ventral tongue	
	3355	Y				M	65	tongue	
	3361	Y				M	57	tongue	
	3364	Y				M	63	tongue	
	3366	Y				F	72	tongue	
	3367	Y				F	88	maxillary alveolus	
	3379	Y				M	63	buccal	
	4012	Y				M	57	tonsil	
	4035	Y				F	63	mandibular alveolus	

*Y indicates that a sample was available for analysis.
†Type of whole genome analysis performed on this sample (if any). *OSCC*, oral squamous cell carcinoma; *WGA*, whole genome analysis; *LG-PVL*, low grade proliferative verrucous leukoplakia; *PVL*, proliferative verrucous leukoplakia; *WES*, whole exome sequencing; *WGMP*, whole genome methylation profiling; *FOM*, floor of mouth; *BOT*, base of tongue; *cOSCC*, conventional OSCC.

Duplicate hybridization was performed for 3 of 4 PVL-OSCC, 1 of 3 cOSCC, and 2 of 4 LG-PVL samples. Arrays were scanned using Illumina's iScan technology, and the data was transferred to the Computational Biological Facility, University of Liverpool.

Preprocessing and normalization. The EPIC arrays were analyzed using functionality within the minfi software package (http://bioconductor.org/packages/release/bioc/html/minfi.html).[15] Briefly, samples were checked for global hybridization quality based on an

average detection value threshold of $P < .05$ for all probes. Individual CpG probes were discarded from the array if their detection value was $P > .01$, indicating a failed position. Probes were also discarded if located on chromosomes X and Y, within 2 base pairs of a single nucleotide polymorphism with a minor allele frequency >0.05, or if the probe was previously found to cross hybridize to multiple genomic locations.[16,17] Sample-wise normalization was performed using the regression of correlated probes algorithm to correct for biases between type I and II probe distributions.[18]

Differential methylation. Univariate statistical analysis for each CpG was performed using the linear models for the microarray data (limma) package.[19] The duplicate Correlation function was used to estimate the consensus correlation between arrays originating from the same biological donor and was subsequently used as a parameter for the least-squares minimization and curve-fitting (lmFit) function. A contrast matrix was built to implement the linear models with coefficients for "PVL-OSCC and cOSCC" and "PVL-OSCC and LG-PVL." Significance was determined based on a Benjamini−Hochberg value-adjusted false-discovery rate (FDR) <0.05. Differential methylation was assessed in the context of regions using DMRcate software.[20] Regions were defined as blocks of 1000 nucleotides for which a Gaussian kernel smoothed function is fit. A region was considered to be differentially methylated if it had a Benjamini−Hochberg value-corrected FDR <0.1 and an absolute mean beta fold change >0.1.

Analysis. All principal component analysis (PCA) was performed using R version 4.0.2 software (R Foundation for Statistical Computing, Vienna, Austria). M values were centered and scaled before matrix decomposition using the *prcomp* function from the stats package.[21] Heatmaps were generated using the *pheatmap* function within the pheatmap package.[22] All hierarchical clustering was performed using the ward. D2 method. Statistical analysis was performed to test the association between principal components and variables in the data using one-way variance analysis. If there was a significant difference for the main effect ($P < .05$), a Tukey's Honest Significant Difference post-hoc comparison was applied. The significance for post-hoc testing was an adjusted $P < .05$.

Single Gene Assays

Somatic variants. Pyrosequencing assays for selected PVL-OSCC- and cOSCC-specific somatic changes were designed using Oligo Primer Analysis Software 7.0 (Molecular Biology Insights Inc [DBA Oligo, Inc], Colorado Springs, CO, USA). Oligonucleotides were synthesized by Eurofins Genomics (Ebersberg, Germany) (Supplemental Table S1). Pyrosequencing was performed on 3 DNA samples from the WES cohort plus an additional 12 PVL-OSCC, 13 LG-PVL, and 20 cOSCC FFPE specimens (Table I) using Pyromark Gold Q24 reagents (Qiagen) on a Pyromark Q96 workstation (Qiagen) and the resulting programs analyzed for the presence of variants at the given site.

Promoter methylation. The DNA was converted with sodium bisulfite using the EZ DNA Methylation-Gold Kit (Zymo Research Corp, Irvine, CA, USA). Quantitative methylation-specific polymerase chain reaction (qMSP) and pyrosequencing methylation (PMA) assays were designed using Oligo 7.0 (Molecular Biology Insights Inc [DBA Oligo, Inc], Colorado Springs, CO, USA) and PyroMark Assay Design SW version 2.0 software (Qiagen), respectively. Oligonucleotides were synthesized by Eurofins Genomics (Supplemental Table S1). As previously described, lymphocyte DNA samples artificially methylated to 20%, 10%, 5%, and 2.5% were used as standards.[23]

A previously published method was used for qMSP of the *CDKN2A* (p16) promoter.[23] DNA from 12 PVL-OSCC and 11 cOSCC samples were analyzed. Assays were multiplexed with *ACTB* as an internal normalization control and run in duplicate. The mean C_t value from the duplicates was used to calculate relative quantitation values using the ΔΔCt method, with the unmethylated lymphocyte DNA being used as the reference, and relative quantitation was compared to the standards to obtain a semi-quantitation of DNA methylation. For PMA of the *MGMT* promoter, polymerase chain reaction products from 20 PVL-OSCC and 20 cOSCC FFPE specimens were subject to pyrosequencing using Pyromark Gold Reagents (Qiagen) on a Pyromark Q96 workstation (Qiagen) and the resulting programs analyzed for the presence of methylation as previously described.[24]

Statistical analysis. The Student's t-test was performed to compare PVL-OSCC and cOSCC variant frequencies.

RESULTS

Whole Exome Sequencing

Seven genes were identified as having PVL-OSCC−specific mutations, defined as being present in at least 3 out of 5 samples (Table II). Two genes (*NOTCH1* and *PIK3CA*) are also commonly mutated in cOSCC. Analysis of the WES data for alterations in other genes mutated at a frequency >15% in conventional OSCCs revealed changes in PVL-OSCC samples at lower frequencies (Table II).

Table II. Most Frequent Genetic Changes in PVL-OSCC and Conventional OSCC

Gene name	*Frequency in PVL-OSCC (this study n = 5)*	*Frequency in OSCC* (n = 311)*
LRP2	80% (4†)	0
LRP5	80% (4)	0
TTN	60% (3)	0
NOTCH1	60% (3)	21.5% (66)
PIK3CA	60% (3)	16.9% (52)
JMJD1C	60% (3)	0
EPG5	60% (3)	0
TP53	40% (2)	78.2% (240)
FAT1	40% (2)	29.3% (90)
CDKN2A	20% (1)	26.1% (80)

*Data generated by The Cancer Genomic Atlas Research Network.[25]
†Number of samples showing somatic changes.
PVL, proliferative verrucous leukoplakia; *OSCC*, oral squamous cell carcinoma.

The genetic changes observed in the *TTN, LRP2, LRP5, JMJD1C*, and *EPG5* genes in PVL-OSCC samples were classified as moderate-low impact because they either produced amino-acid changes with limited structural effect or no amino-acid change (Supplemental Table S2). However, the changes observed in *NOTCH1 a*nd *PIK3CA* were classified as high impact because they produced amino-acid changes that altered protein secondary and/or tertiary structure or inserted a stop codon. Analysis of mutation profiles demonstrated the presence of mostly novel genetic alterations in the PVL-OSCC samples and the absence of more commonly observed mutations (Columns 1 and 3 in Table III). The only 2 mutations observed in both the PVL-OSCC and cOSCC samples were at *PIK3CA* p.E545K, a mutation found in approximately 9% of all cancers annotated in TGCA, and *NOTCH1* p.R353C, a mutation found at low frequency in both PVL-OSCC and cOSCC.

Pyrosequencing assays were designed to cover *PIK3CA* p.E545K and p.E542K mutations, the *PIK3CA* p.H1047R mutation, and *NOTCH1* p.G326D and p.C387X/p.C387Y mutations. Samples for pyrosequencing included DNA from specimens used to generate the primary WES data, LG-PVL, to assess early- and late-stage appearance, and cOSCC samples. In this larger cohort, the frequency of mutation for *PIK3CA* p.E545K fell to levels comparable to those observed in conventional OSCC ($P > .05$) (Table III). Notably, 2 of 3 of the LG-PVL samples demonstrating *PIK3CA* p.E545K mutations also showed that mutation in the corresponding PVL-OSCC tissue.

Whole Genome Methylation Profiling

Global PCA. The principal component analysis assessed variance based on methylation profiles among PVL-OSCC, cOSCC, and LG-PVL tissue samples. Principal component analysis, based on unbiased, genome-wide methylation profiles of ~785,000 probes, demonstrated significant differences in variance within principal component 1 (PC1) between LG-PVL and cOSCC tissue ($P = .026$) and between LG-PVL and PVL-OSCC tissue ($P = .005$) (Figure 1). However, no significant differences in variance were observed between cOSCC and PVL-OSCC in PC1 or later components, indicating similar global methylation patterns in the 2 tissues.

Table III. Single Mutations Screened in PVL Samples

Gene name	*Mutation*	*Frequency in PVL-OSCC*		*Frequency in conventional OSCC*		*Frequency in LG-PVL*
		WES (n = 5)	*Resequencing*	*TCGA**	*Resequencing (n = 18)*	*Resequencing (n = 13)*
PIK3CA	p.E542K (GAG-GTG)	0	0	8/112 (7%†)	0	0
	p.E545K (GAG-AAG)	2 (40%)	2/15 (13%)	10/112 (9%)	3 (17%)	3 (23%)
	p.H1047R (CAG-CGT)	0	0	11/112 (12%)	NT	0
	p.T1025A (ACC-GCC)	1 (20%)	NT	0	NT	NT
NOTCH1	p.G326D (GGC-GAC)	1 (20%)	1/11 (9%)	0	0	NT
	p.R353C (CGT-TGT)	1 (20%)	NT	1/86 (1%)	NT	NT
	p.C387X (TGC-TGA)	1 (20%)	1/14 (7%)	0	0	NT
	p.C387Y (TGC-TAC)	0	1/14 (7%)	0	0	NT
	p.C627G (TGC-GGC)	1 (20%)	NT	0	NT	NT
	p.Q1247X (CAG-TAG)	1 (20%)	NT	0	NT	NT

*Data from The Cancer Genomic Atlas.[25]
†Indicates percentage of samples demonstrating the mutation.
PVL, proliferative verrucous leukoplakia; *OSCC*, oral squamous cell carcinoma; *LG*, low grade; *WES*, whole exome sequencing; *TCGA*, The Cancer Genomic Atlas; *NT*, not tested

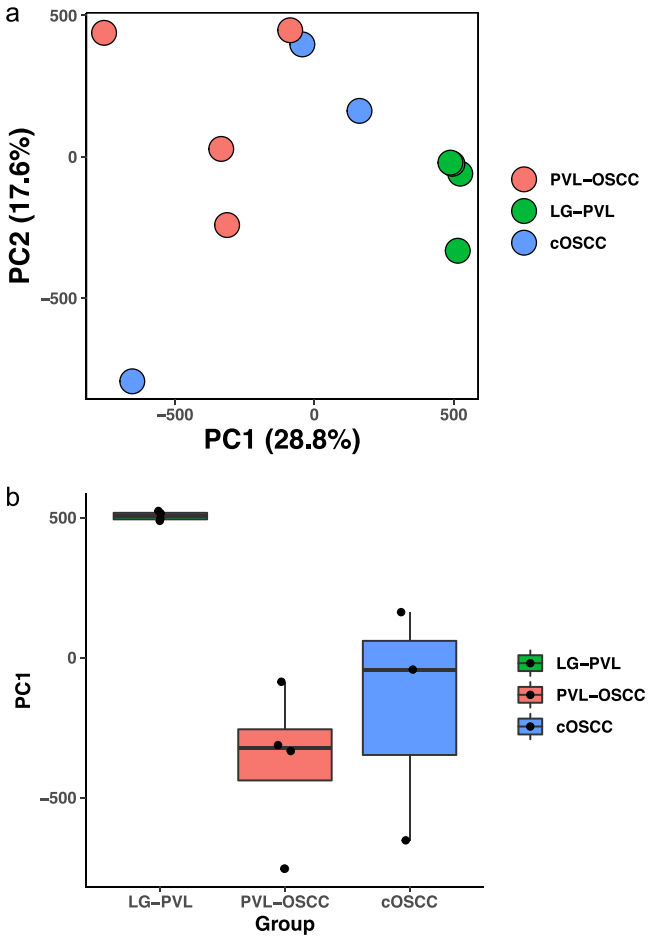

Fig. 1. Unbiased analysis of genome-wide methylation differences among conventional OSCC, low grade proliferative verrucous leukoplakia, and proliferative verrucous leukoplakia oral squamous cell carcinoma . (A) Principal component analysis. (B) Box-and-whisker plot of data from principal component 1.

Univariate models. A total of 63 differentially methylated probes (DMPs) between PVL-OSCC and cOSCC samples were identified using a univariate model in limma with a Benjamini−Hochberg FDR <0.05. (Supplementary Table S3). Proportional to the distribution of probes tested on the EPIC array, the 63 differentially methylated probes contain 1.7-fold enrichment for probes located within CpG islands, with 42 of 63 probes located within a coding region of a gene. A further 19 regions were identified based on defined blocks of 1000 nucleotides within the 63 CpGs to be differentially methylated (DMRs) based on an FDR of 10%. (Supplementary Table S4). Interestingly, the promoters of genes commonly methylated in cOSCC, such as *CDKN2A*, were absent from both lists.

Targeted multivariate clustering and PCA. Multivariate unsupervised hierarchical clustering and PCA showed that LG-PVL, PVL-OSCC, and cOSCC could be discriminated by the methylation profiles of the 63 differentially methylated loci (Figure 2A). Interestingly, this analysis grouped LG-PVL more closely with cOSCC than with PVL-OSCC. Moreover, using only the 63 probes identified from the univariate model, PC1 and PC2 were shown to capture approximately 90% variance and to be significantly associated with tissue type (Figure 2B), with PC1 separating PVL-OSCC from cOSCC and PC2 separating LG-PVL from both OSCC tissue types. Low-grade PVL was grouped more closely to cOSCC than PVL-OSCC in PC1. However, 16 of the 63 differentially methylated loci showed little or no difference in methylation levels between PVL-OSCC and LG-PVL, which may be early events in the development of PVL-OSCC (Supplementary Table S5). Seven of the 16 DMPs are located in a CpG island, of which 4 are associated with known genes (*MACF1, SFRP2, LMX1A,* and *ME3).*

Gene ontology. The 63 differentially methylated probes were analyzed for overlapping biological processes. Differences in methylation were most

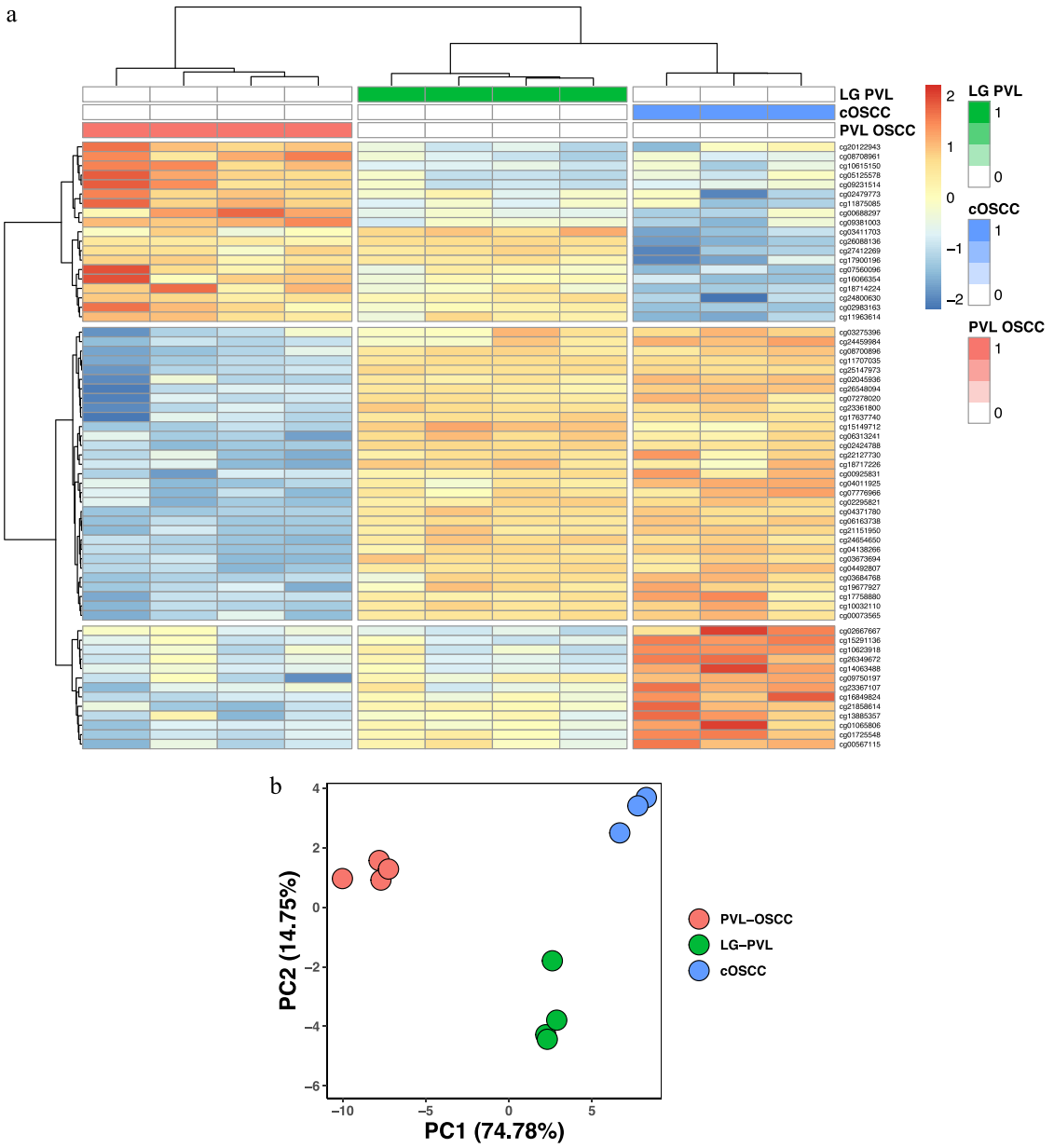

Fig. 2. Multivariate clustering using 63 differentially methylated probes. (A) Unsupervised hierarchical clustering based on scaled M values of methylation at 63 differentially methylated probes. (B) Principal component analysis of the 63 differentially methylated probes.

significant for divalent metal ion transport, particularly calcium movement (Supplementary Table S3). Interestingly, these gene promoters were generally less methylated in PVL-OSCC compared with cOSCC.

Analysis of gene promoters commonly methylated in OSCC. None of the gene promoters commonly hypermethylated in cOSCC were identified in the list of probes that were differentially methylated between PVL-OSCC and cOSCC (Supplementary Tables S3 and S4). This observation implies that the methylation levels at these promoters are similar in PVL-OSCC and cOSCC. To investigate this further, multivariate unsupervised hierarchical clustering was performed using 315 probes representing 24 genes shown to have significantly altered promoter methylation in OSCC[26,27] (Supplementary Table S6). This confirmed the separation of LG-PVL tissue from all cancer tissue and suggested that, despite many similarities in the methylation profiles of PVL-OSCC and cOSCC, there were also some differences (Figure 3).

In addition, the methylation status of the *CDKN2A* (p16) promoter was investigated by RT-qMSP[23] and the promoter of *MGMT* by PMA[24] in DNA prepared

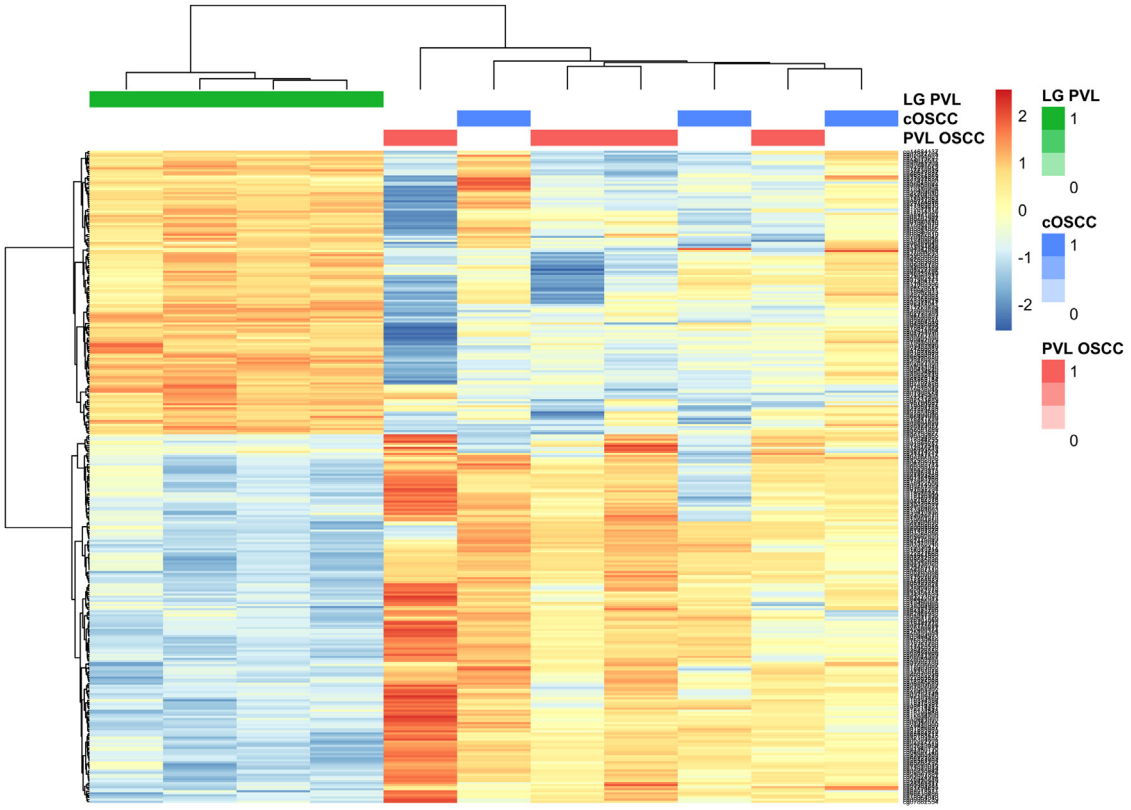

Fig. 3. Multivariate clustering using 315 probes associated with differentially methylated genes identified from the literature. Unsupervised hierarchical clustering based on scaled M values of methylation.

from FFPE tissue. None of the PVL-OSCC samples demonstrated *CDKN2A* promoter methylation compared with 5 of 9 (56%) cOSCC samples (P = .013). Similarly, only 3 of 18 (17%) of the PVL-OSCC samples showed *MGMT* promoter methylation compared with 5 of 18 (28%) of the cOSCC samples, but this difference was not statistically significant (P = .33).

DISCUSSION

Proliferative verrucous leukoplakia transforms into OSCC at a frequency >50% in comparison with 10% for mild to moderate OED and 24% for severe OED and carcinoma in situ.[5,6] Historically, molecular studies have attempted to show that the molecular profile of PVL-OSCC is similar to that of cOSCC. In contrast, we aimed to investigate the differences between these 2 entities to explain the differences in their transformation rates.

In this study, whole exome sequencing identified 7 genes presenting with mutations in ≥60% of samples, only 2 of which (*PIK3CA* and *NOTCH1*) had previously been identified as commonly mutated in cOSCC.[25] In contrast, *TP53* mutations were less common in the cohort examined. Of course, these data may simply reflect the small sample examined, but the *TP53* data reflect previous observations in PVL.[28] The *PIK3CA* mutations identified in PVL-OSCC tumors were different from those most commonly observed in cOSCC but had been previously shown to have pathogenic potential in other cancers, most notably breast and endometrium.[29] The p.T1025A alteration located in the PI3K/PI4K domain of the protein has been shown to increase transforming ability in cell lines in culture and is predicted to be a gain of function mutation.[30] The p.E545K alteration, which is located in the helical domain and commonly observed in many cancers, results in an amino-acid substitution of the opposite charge that uncouples the catalytic and regulatory subunits of the protein,[31] as does the p.E542K mutation more commonly observed in head and neck cancer. Interestingly, the p.E545K mutation has also been shown to alter fatty-acid metabolism, including the upregulation of arachidonic acid, which is needed to synthesize prostaglandins, a pro-inflammatory molecule implicated in cancer development.[32] Thus, the p.E545K mutation may be more important than the p.E542K alteration in the pathogenesis of transformation. The p.E545K mutations of *PIK3CA* were also observed in early LG-PVL lesions in our study, which suggests that this oncogenic driver is an early occurring event. However, there is no support in the literature for the role of early mutation of *PIK3CA* in OED.

NOTCH1 alterations can be oncogenic or tumor suppressive in head and neck SCC.[33] The mutations observed in this study are all located in the extracellular subunit and may affect receptor binding, with 2 changing cysteine residues potentially affecting the secondary and the tertiary structure that relies on disulfide bonding.

Methylation profiling comparing PVL-OSCC with non-malignant LG-PVL identified 157,963 differentially methylated probes and 26,498 differentially methylated regions. If the list is restricted to promoters (located -1500 to -200bp upstream from the start site and within the 5′UTR), then 4,871 islands were identified as differentially methylated. This is similar to that described by Herreros-Pomares et al.,[10] who identified 4,647 DMRs in a series of 10 PVL samples compared with 5 healthy tissue samples. However, there were no common targets in the top 50 DMRs from our and Herreros-Pomares' data sets. Herreros-Pomares also showed similarities in the methylation profiles of premalignant PVL and that of cOSCC in the TCGA for 13 differentially methylated, differentially expressed probes. In contrast, the data in the current study identified differences in the methylation profiles of PVL-OSCC and cOSCC. Unsurprisingly, none of the 63 DMPs that are differentially methylated were identified by Herreros-Pomares as having similar methylation profiles in PVL-OSCC and cOSCC.

It may be postulated that DMPs differentially expressed in PVL-OSCC compared with cOSCC that also show similar methylation levels in comparing LG-PVL with PVL-OSCC, indicate early events in the transformation process. Of the 4 known genes that fell into this group, only *MACF1* showed a methylation pattern consistent with tumor development. This microtubule-associated protein is implicated in proliferation, migration, and cell signaling in several cancers[34] and showed reduced methylation in PVL-OSCC. In contrast, reduced expression of *SFRP2* and *LMX1A* have been previously associated with colorectal and bladder cancer, respectively,[35,36] but both showed decreased methylation in PVL samples in this study. Similarly, *ME3* shows increased expression in pancreatic cancer[37] but was characterized by increased methylation in the PVL samples in this study. It is well known that methylation status does not always negatively correspond with expression and it should be noted that the relative levels of methylation reported in the current study are compared with cOSCC and not with normal tissue. Nevertheless, the implication is that *MACF1* is a gene worthy of further study in developing PVL-OSCC.

Global hypomethylation coupled with targeted promoter hypermethylation is a key feature of OSCC.[38,39] Subtle differences between OSCC populations have been documented,[40] so it is unsurprising that we identified differences between the methylation patterns in PVL-OSCC and cOSCC. None of these differences in methylation were in gene promoters commonly methylated in cOSCC; thus, we hypothesized that these were critical and common to the transformation process in all oral cancer. However, multivariate unsupervised hierarchical clustering of 315 probes representing 24 genes shown to have significantly altered promoter methylation in both our previous study[26] and several candidate gene studies[27] showed differences between PVL-OSCC and cOSCC methylation patterns. Interestingly, comparatively lower levels of methylation were observed in PVL-OSCC compared with cOSCC for several of these probes, which we validated in the *CDKN2A* gene promoter. This suggests that different mechanisms are involved in developing PVL-OSCC compared with cOSCC.

Gene ontology analysis of the 63 differentially methylated probes identified divalent metal ion transport, particularly calcium movement, and other signaling pathways as being affected. However, the gene promoters were generally less methylated in PVL-OSCC than in cOSCC, suggesting increased expression of these pathways. Nevertheless, the pattern was not uniform, with some pathway members being hypermethylated in cOSCC and others in PVL-OSCC. Calcium movement is associated with intracellular signaling, which is often activated in cancer, but this is not the only role of this cation. Increased calcium in the mitochondria can stimulate the calcium-sensitive dehydrogenases of the Krebs cycle, leading to increased ATP production and release of superoxides,[41] which may stimulate proliferation and DNA damage, respectively.

In conclusion, we identified specific differences in the mutation and methylation profiles of PVL-OSCC and cOSCC, suggesting differences in the transformation pathway in these 2 entities. However, we could not identify a single genetic or epigenetic pathway or gene unique to PVL. Although we based our data on only a few samples, we carefully curated them for a clinical and pathologic diagnosis of PVL, and we augmented them with samples from premalignant, low-grade PVL. Further studies should concentrate on the analysis of these earlier lesions to identify markers of transformation that may also apply to more common oral premalignant disorders, such as oral epithelial dysplasia.[42]

FUNDING

EMO was supported by the Academic Staff Training and Development Programme (TETFund), Lagos State University, Ojo, Nigeria (LASU/VC/TETF/ASTandD/001); the British Association of Oral and Maxillofacial Surgeons; the University of Liverpool PhD bursary;

and the University of Liverpool Technology Directorate Voucher (40428830). The funding sources had no role in the study design, collection and analysis of data, writing of the manuscript, or decision to publish.

DECLARATION OF INTEREST

None.

SUPPLEMENTARY MATERIALS

Supplementary material associated with this article can be found in the online version at doi:10.1016/j.oooo.2023.03.004.

REFERENCES

1. Hansen LS, Olson JA, Silverman SJ. Proliferative verrucous leukoplakia. A long-term study of thirty patients. *Oral Surg Oral Med Oral Pathol*. 1985;60:285-298.
2. Silverman SJ, Gorsky M. Proliferative verrucous leukoplakia: a follow-up study of 54 cases. *Oral Surg Oral Med Oral Pathol Oral Radiol Endod*. 1997;84:154-157.
3. Gonzáles-Moles MÁ, Warnakulasuriya S, Ramos-García P. Prognosis parameters of oral carcinomas developed in proliferative verrucous leukoplakia: a systematic review and meta-analysis. Cancers (Basel). 2021;13:4843.
4. Akrish S, Ben-Izhak O, Sabo E, Rachmiel A. Oral squamous cell carcinoma associated with proliferative verrucous leukoplakia compared with conventional squamous cell carcinoma – a clinical, histologic and immunohistochemical study. *Oral Surg Oral Med Oral Pathol Oral Radiol*. 2015;119:318-325.
5. Ramos-García P, Gonzáles-Moles MÁ, Mello FW, Bagan JV, Warnakulasuriya S. Malignant transfromation of oral proliferative verrucous leukoplakia: a systematc review and meta-analysis. *Oral Dis*. 2021;27:1896-1907.
6. Mehenna HM, Rattay T, Smith J, McConkey CC. Treatment and follow-up of oral dysplasia – a systematic review and meta-analysis. *Head and Neck*. 2009;31:1600-1609.
7. Borgna SC, Clarke PT, Schache AG, et al. Management of proliferative verrucous leukoplakia: justification for a conservative approach. *Head and Neck*. 2017;39:1997-2003.
8. Okoturo EM, Risk JM, Schache AG, Shaw RJ, Boyd MT. Molecular pathogenesis of proliferative verrucous leukoplakia: a systemic review. *Br J Oral Maxillofac Surg*. 2018;56:780-785.
9. Rintala M, Vahlberg T, Salo T, Rautava J. Proliferative verrucous leukoplakia and its tumor markers: systematic review and meta-analysis. *Head and Neck*. 2019;41:1499-1507.
10. Herreros-Pomares A, Llorens C, Soriano B, Bagan L, et al. Differentially methylated genes in proliferative verrucous leukoplakia reveal potential malignant biomarkers for oral squamous cell carcinoma. *Oral Oncol*. 2021;116:105191.
11. Llorens C, Soriano B, Trilla-Fuertes L, et al. Immune expression profile identification in a group of proliferative verrucous leukoplakia patients: a pre-cancer niche for oral squamous cell carcinoma development. *Clin Oral Invest*. 2021;25:2645-2657.
12. Shaw RJ, Hobkirk AJ, Nikolaidis G, et al. Molecular staging of surgical margins in oral squamous cell carcinoma using promoter methylation of $p16^{INK4A}$, cytoglobin, E-cadherin, and *TMEFF2*. *Ann Surg Oncol*. 2013;20:2796-2802.
13. Li H, Durbin R. Fast and accurate short read alignment with Burrows–Wheeler transform. *Bioinformatics*. 2009;25:1754-1760.
14. Kim S, Scheffler K, Halpern AL, et al. Strelka2: fast and accurate calling of germline and somatic variants. *Nature Methods*. 2018;15:591-594.
15. Aryee MJ, Jaffe AE, Corrada-Bravo H, et al. Minfi: a flexible and comprehensive Bioconductor package for the analysis of Infinium DNA methylation microarrays. *Bioinformatics*. 2014;30:1363-1369.
16. Chen YA, Lemire M, Choufani S, et al. Discovery of cross-reactive probes and polymorphic CpGs in the Illumina Infinium HumanMethylation450 microarray. *Epigenetics*. 2013;8:203-209.
17. Pidsley R, Zotenko E, Peters TJ, et al. Critical evaluation of the Illumina MethylationEPIC BeadChip microarray for whole-genome DNA methylation profiling. *Genome Biol*. 2016;17:208.
18. Niu L, Taylor JA. RCP: a novel probe design bias correction method for Illumina Methylation BeadChip. *Bioinformatics*. 2016;32:2659-2663.
19. Ritchie ME, Phipson B, Wu D, et al. Limma powers differential expression analysis for RNA-sequencing and microarray studies. *Nuc Acids Res*. 2015;43:e47.
20. Peters TJ, Buckley MJ, Statham AL, et al. De novo identification of differentially methylated regions in the human genome. *Epigenetics and Chromatin*. 2015;8:6.
21. RCoreTeam. R: a language environment for statistical computing. R Foundation for Statistical Computing, Vienna. Available at: https://www.R-project.org.
22. Kolde R. Pheatmap: pretty heatmaps. R package version 1.0.12. Available at: https://cran.r-project.org/web/packages/pheatmap/index.html.
23. Nikolaidis G, Raji O, Markopoulou S, et al. DNA methylation biomarkers offer improved diagnostic efficiency in lung cancer. *Cancer Res*. 2012;72:5692-5701.
24. Shaw RJ, Hall GL, Lowe D, et al. CpG island methylation phenotype (CIMP) in oral cancer: associated with a marked inflammatory response and less aggressive tumour biology. *Oral Oncol*. 2007;43:878-886.
25. National Cancer Institute. National Cancer Institute GDC Data Portal. Available at: https://portal.gdc.cancer.gov. Accessed 05 13, 2022.
26. Jithesh PV, Risk JM, Schache AG, et al. The epigenetic landscape of oral squamous cell carcinoma. *Br J Cancer*. 2013;108:370-379.
27. Mascolo M, Siano M, Ilardi G, et al. Epigenetic disregulation in oral cancer. *Int. J. Mol. Sci.* 2012;13:2331-2352.
28. Gopalakrishnan R, Weghorst CM, Lehman TA, et al. Mutated and wild-type p53 expression and HPV integration in proliferative verrucous leukoplakia and oral squamous cell carcinoma. *Oral Surg Oral Med Oral Pathol Oral Radiol Endod*. 1997;83:471-477.
29. Tate JG, Bamford S, Jubb HC, et al. COSMIC: the Catalogue Of Somatic Mutations in Cancer. *Nuc Acids Res*. 2019;47:D941-D947.
30. Ng PK, Li J, Jeong KJ, et al. Systemic functionnal annotation of somatic mutations in cancer. *Cancer Cell*. 2018;33:450-462.
31. Leontiadou H, Galdadas I, Athanasiou C, Cournia Z. Insights into the mechanism of the *PI3CA* E545K activating mutation using MD simulations. *Sci Rep*. 2018;8:15544.
32. Koundouros N, Karali E, Tripp A, Valle A, Inglese P, Perry NJS, et al. Metabolic fingerprinting links oncogenic *PIK3CA* with enhanced arachidonic acid-derived eicosanoids. *Cell*. 2020;181:1596-1611.
33. Fukusuki T, Califano J. The NOTCH pathway in head and neck squamous cell carcinoma. *J Dent Res*. 2018;97:645-653.
34. Miao Z, Ali A, Hu L, et al. Microtubule actin cross-linking factor 1, a novel potential target in cancer. *Cancer Sci*. 2017;108:1953-1958.
35. Zhang H, Qi J, Wu Y-Q, et al. Accuracy of early detection of colorectal tumours by stool methylation markers: a meta-analysis. *World J Gastroenterol*. 2014;20:14040-14050.
36. Zhao Y, Guo S, Sun J, et al. Methylcap-Seq reveals novel DNA methylation markers for the diagnosis and recurrence prediction

of bladder cancer in a Chinese population. *PLoS ONE*. 2012;7: e35175.
37. Zhang Q, Li J, Tan XP, Zhao Q. Effects of ME3 on the proliferation, invasion and metastasis of pancreatic cancer cells through epithelial-mesenchymal transition. *Neoplasma*. 2019;66:896-907.
38. Foy J-P, Pickering CR, Papadimitrakopoulou V, et al. New DNA methylation markers and global DNA hypomethylation are associated with oral cancer development. *Cancer Prev Res*. 2015;8:1027-1035.
39. Chatterjee R, Das S, Chandra A, Basu B. Epigenome-wide DNA methylation profiles in oral cancer. In: Wei LK, ed. *Computational Epigenetics and Diseases*, London, UK: Academic Press; 2019:213-231.
40. Basu B, Chakraborty J, Chandra A, et al. Genome-wide DNA methylation profile identified a unique set of differentially methylated immune genes in oral squamous cell carcinoma patients in India. *Clin Epigenetics*. 2017;9:13.
41. McCormack JG, Halestrap AP, Denton RM. Role of calcium ions in regulation of mammalian intramitochondrial metabolism. *Physiol Rev*. 1990;70:391-425.
42. Morandi L, Gissi D, Tarsitano A, et al. CpG location and methylation level are crucial factors for the early detection of oral squamous cell carcinoma in brushing samples using bisulfite sequencing of a 13-gene panel. *Clin Epigenetics*. 2017;9:85.